Experimental and Theoretical Evidence of C—H···O Hydrogen Bonding in Liquid 4-Fluorobenzaldehyde

Paulo J. A. Ribeiro-Claro,*[a] M. Paula M. Marques,[b, c] and Ana M. Amado[b]

The presence of C—H···O hydrogen bonds in liquid 4-fluorobenz-aldehyde has been studied by a combination of theoretical and spectroscopic methods. Ab initio calculations yielded bond energies and preferred bonding geometries, and the calculated spectroscopic properties have been compared with the experimental results.

The presence of C—H···O hydrogen bonds in the liquid phase is strongly supported by vibrational and NMR spectroscopic data.

Particular attention is paid to the spectroscopic effects related to the predicted shortening of the C—H bond engaged in the C—H···O contact. The concentration-dependent intensity in the C—H stretching region is tentatively assigned to a blue-shift effect due to C—H···O hydrogen bonding.

KEYWORDS:

ab initio calculations · hydrogen bonds · NMR spectroscopy · vibrational spectroscopy ·

Over the last few years, the role of the C—H···O hydrogen bond in crystal engineering and molecular recognition processes has aroused considerable interest.[1–4] The small binding energy of this interaction, when compared with conventional O—H···O hydrogen bonds, seems to be overcome by the almost ubiquitousness of C—H bonds and efficient cooperativity effects.

Despite all the recent interest in the subject, the nature of the C—H···O hydrogen bond is still controversial.[5, 6] One of its most peculiar features—the shortening of the C—H covalent bond upon hydrogen bonding—is not yet fully understood. The behavior of the C—H bond length is opposite to that found for conventional O—H(···X) donor bonds (except for strongly acidic C—H(···X) donors, such as terminal alkynes). Although there is a convincing amount of data from ab initio calculations describing the shortening of the C—H bond,[3, 5–7] experimental evidence of such an effect is still scarce.[8–13] In fact, since most of the experimental evidence for C—H···O hydrogen bonds come from X-ray structure determinations, the spectroscopic properties of this type of hydrogen bond deserve further attention.

Previous reports have shown that the presence of C—H···O hydrogen bonds in the liquid phase of methoxy- and ethoxy-benzaldehyde derivatives can be inferred from both vibrational and NMR spectroscopic studies.[10, 11] The engagement of the carbonyl oxygen atom in the hydrogen bond becomes evident from the splitting of the carbonyl stretching mode and from the ^{17}O NMR chemical shift. The C—H donor is not as easy to identify, but some spectroscopic data suggesting the participation of aldehydic, aromatic, and alkoxy C—H bonds have been found.[10, 11]

In this work, a combined theoretical and spectroscopic study of C—H···O hydrogen bonds in liquid 4-fluorobenzaldehyde (4FB) is reported using ab initio calculations, and vibrational and NMR spectroscopy. The purpose of this study was twofold: firstly, to describe the C—H···O interactions in terms of bonding energies and preferred geometries; secondly, to characterize the spectroscopic effects of the C—H···O hydrogen bonding, paying particular attention to those related to the shortening of the C—H bond length.

Results and Discussion

### Theoretical Study of the Dimerization Process

Ab initio calculations have proven to be a valuable tool for predicting dimer structures and other relevant molecular parameters, such as atomic charges, bond orders, and the strength and energetic contribution of the intermolecular interactions. In addition, the vibrational frequencies and, more recently, NMR shifts associated with the dimerization process can be accurately predicted.[14–17]

[a] Prof. P. J. A. Ribeiro-Claro
Departamento de Química
Universidade de Aveiro
3810-193 Aveiro (Portugal)
Fax: (+351) 234-370-084
E-mail: pclaro@dq.ua.pt

[b] Dr. M. P. M. Marques, A. M. Amado
Unidade I&D "Química-Física Molecular"
Departamento de Química, FCTUC
Universidade de Coimbra
3004-535 Coimbra (Portugal)

[c] Dr. M. P. M. Marques
Departamento de Bioquímica, FCTUC
Universidade de Coimbra
3001-401 Coimbra (Portugal)

Figure 1 shows the optimized geometries of the five most significant dimer configurations of 4FB, at both the HF/6-31G* and B3LYP/6-31G* levels. The hydrogen bond distances and bond angles calculated at the B3LYP level are indicated in each case. Table 1 lists the hydrogen bonding energies of the optimized dimers **1** to **5**.
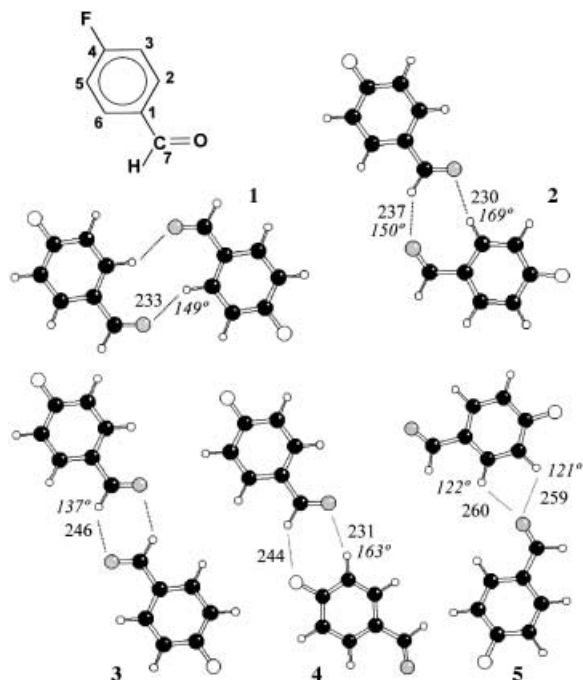
Figure 1. Chemical structure of 4FB, showing the atom numbering used throughout the text, and the B3LYP/6-31G optimized geometries for the five lowest energy minima of 4FB dimers. Hydrogen bond distances are given in picometers, C—H···O angles in degrees. The calculated dimerization energies can be found in Table 1.*

Table 1. *Dimerization energies (Dimer − 2 × Monomer) $\Delta E_{dimerization}$ [kJ mol^{-1}] and relative energies of 4FB dimers.*

Dimer[a]	1	2	3	4	5
HF/6-31G*	− 17.0	− 17.3	− 16.7	− 13.7	− 11.1
B3LYP/6-31G*	− 21.8	− 20.7	− 18.2	− 18.8	− 13.5
after ZPVE[b]	− 19.2	− 17.9	− 15.4	− 16.4	− 11.8
after CP[c]	− 12.0	− 11.5	− 9.2	− 8.2	− 7.1
after CP + ZPVE[b,c]	− 9.3	− 8.6	− 6.4	− 5.8	− 5.4

Absolute energy (B3LYP/6-31G*) of form **1** is − 889.622739258 E_h. [a] Dimer numbered in accordance with Figure 1. [b] ZPVE = zero point vibrational energy. [c] CP = counterpoise correction.

The five dimer structures reported above are those displaying a dimerization energy < -5 kJ mol^{-1}. In fact, since each 4FB molecule presents five potential H-donors (all the C—H bonds) and three potential H-acceptors (the carbonyl oxygen, fluorine atom, and aromatic π-system), the possible donor/acceptor combinations yielded more than twenty starting geometries for the 4FB dimers. In addition, π-stacking and dipole alignment structures have also been tested as dimerization options, but they either resulted in low stability minima or fell to one of the

previous hydrogen-bonded forms during the geometry optimization. However, at the MP2/6-31G** level, which is expected to provide a better description of the π-stacking interactions, C—H···O bonded dimers are no longer the most stable ones (for example, the absolute energies of dimer **1** and a π-stacked dimer are − 887.098591 E_h and 887.099761 E_h, respectively).

At the Hartree–Fock (HF) level, the bare (uncorrected) dimerization energies are in the range 11.1 – 17.3 kJ mol^{-1}. Dimer **2** was calculated to be the lowest energy minimum, with dimers **1** and **3** lying just 0.3 and 0.6 kJ mol^{-1} above, respectively.

The uncorrected B3LYP dimerization energies are higher than their HF counterparts (13.5 – 21.8 kJ mol^{-1} range), but, when corrected for both the zero-point vibrational energy (ZPVE) and the basis set superposition error (BSSE), the values dropped to the 5.4 – 9.3 kJ mol^{-1} range. At this level, the stability order of dimers **1** and **2** is inverted, with dimer **1** becoming more stable than dimer **2** by about 1 kJ mol^{-1}. In addition, the symmetric dimer **3** becomes significantly less stable, approaching the energy of structures **4** and **5**.

These results (Figure 1 and Table 1) allow some conclusions, regarding the nature of preferred donor and acceptor groups in 4FB, to be drawn. As expected, the carbonyl oxygen atom is a more efficient proton acceptor than fluorine. All the dimer forms presenting C—H···F contacts were found to be less stable than those based on C—H···O interactions. Regarding the C—H donors, the ring C_2—H group gives rise to the most stabilizing C—H···O interaction, as can be seen by comparing the dimerization energy along the series **1** →**2** →**3**.

The same general conclusion was obtained from the calculated intermolecular distances. As can be seen from Figure 1, the C_{ring}—H···O distance is always significantly shorter than the two other types of C_7—H···O interactions predicted in the dimers presented. There is an almost linear correlation between the C—H···O distance and the C—H···O angle, which reflects the directionality of the hydrogen-bonding nature of the interaction. The exception observed for structure **1**, which presented a C—H···O angle about 10° narrower than that expected from the previous correlation, seems to be related to the orientation of the lone pairs of the acceptor atom. In fact, a linear C—H···O angle could be achieved with a linear C=H···O angle, but a C=H···O angle more in accordance with an sp^2 hybridized oxygen atom is preferred.

The C—H···F contacts—as observed in dimer **4**—follow the same general behavior (shorter distances for larger angles), with the C—H···F distances generally being about 10 pm longer than the C—H···O ones. On the whole, the calculated dimer geometries reflect an increase of the interaction strength in the order C_{ring}—H···O > C_7—H···O > C_7—H···F > C_{ring}—H···F.

Additional support for this stability order was obtained by a natural bond orbital (NBO) analysis. Table 2 and Figure 2 summarize the NBO results at the B3LYP/6-31G* level, giving the most relevant stabilizing intermolecular energies (above 0.5 kJ mol^{-1}) and the corresponding Wiberg bond orders (Table 2), as well as the predicted changes in atomic charges (dimer relative to monomer) for the representative dimers **1** to **3** (Figure 2).

As can be seen, the C_{ring}—H···O interactions are significantly more stabilizing than the C_7—H···O contacts. The less stabilizing

Table 2. *NBO results (second-order stabilization energy [kJ mol^{-1}] and Wiberg bond orders) for the five most stable optimized dimer structures.[a]*

Dimer	Interaction[b]	Energy[c]	Interaction	Wiberg bond order
1	Lp(O)···σ*C_2—H	14.3	C_2—H···O	0.011
2	Lp(O)···σ*C_2—H	17.6	C_2—H···O	0.017
	Lp(O)···σ*C_7—H	11.4	C_7—H···O	0.009
3	Lp(O)···σ*C_7—H	9.2	C_7—H···O	0.010
4	Lp(O)···σ*C_5—H	17.7	C_5—H···O	0.017
	Lp(F)···σ*C_7—H	6.2	C_7—H···F	0.007
5	Lp(O)···σ*C_5—H	3.8	C_5—H···O	0.005
	Lp(O)···σ*C_6—H	3.1	C_6—H···O	0.003

[a] Atom numbering in accordance with Figure 1. [b] Lp = lone pair. [c] Only interactions greater than 0.5 kJ mol^{-1} are presented.
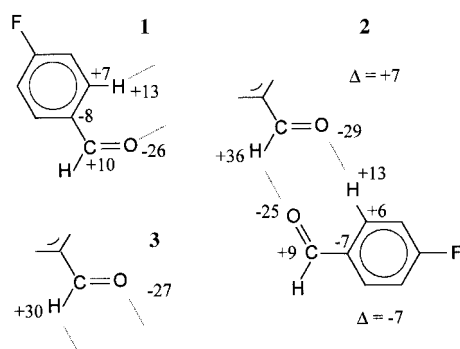
Figure 2. *Atomic charge variation upon dimerization (me) obtained from a natural population analysis. Only values above 5 me are shown.*

intermolecular contacts are those involving the fluorine atom's lone pairs, as in dimer **4**. Similar conclusions are evident by comparing the calculated Wiberg bond orders.

With regard to charge redistribution in the dimers, Figure 2 shows a clear distinction between the formyl and aryl C—H donors, as the gain in positive charge of the hydrogen atom is much larger in the latter. The charge increase on the formyl moiety compares well with the values reported in the literature for the $F_3CH \cdots OCH_2$ hydrogen bonds.[5] In dimer **2**, there is a net charge transfer of -7 me from the top monomer to the bottom monomer (see Figure 2). This net electron transfer arises from the difference between the C_7—H···O and the C_2—H···O hydrogen bonds, with the stronger C_2—H···O partner presumably being responsible for a larger electron density transfer from the proton acceptor to the proton donor molecule.

Ab initio calculations yield relevant information regarding the structural changes that follow the hydrogen bonding process. Particular attention was paid to the bond length changes due to dimerization, since they can manifest themselves in important spectral features. As expected, the involvement of the carbonyl oxygen atom in the hydrogen bonding led to an increase of the C=O bond length of up to 0.6 pm. The largest bond lengthening was observed when the oxygen atom formed a hydrogen bond with the formyl hydrogen atom (dimers **2** and **3**). A similar effect was observed for the C—F bond length (dimer **4**) which showed an increase of 0.8 pm. The behavior of the C—H groups is not as straightforward. In fact, whereas a slight C—H shortening was observed for the hydrogen bonded C_2—H and C_7—H (up to 0.7

and 0.2 pm, respectively), the opposite was predicted for the other C_{ring}—H bonds acting as the H-bond donors, which increased by 0.2 pm.

The above-mentioned structural changes led to some shifts of both the vibrational bands and NMR signals, particularly of those related to the fragments directly involved in the H-bond interaction (for example, C=O and C—H groups). The calculated shifts can be compared with the experimental ones, keeping in mind that calculations refer to isolated systems whereas the experimental results were obtained in the condensed phase.

Table 3 presents the calculated values for the fundamental modes of 4FB, compared with the experimental values (vibrational spectra are shown in Figure 3). The C=O and C—H

Table 3. *Wavenumbers and approximate description of the vibrational modes for 4FB, using a numbering scheme consistent with the Mulliken recommendations and the C_s point group symmetry.*

FTIR	Raman	ab initio[b]		Ring	—CH(=O)
3107	3110	3106[c]		$\nu_{CH\cdots O}$(?)	
3076	3076	3101	ν_1	ν_{CH}	
3056		3099	ν_2	ν_{CH}	
3043	3046	3089	ν_3	ν_{CH}	
3005	3003	3060	ν_4	ν_{CH}	
2849	2848				
2830	2830	2793	ν_5		ν_{CH}
2794	2793				
2741	2742				
1702	1704	1728	ν_6		$\nu_{C=O}$
1692	1697	1718–1714[c]			$\nu_{C=O\cdots H}$
1597	1601	1596	ν_7	ν_{CC}	
		1576	ν_8	ν_{CC}	
1506	1505	1495	ν_9	ν_{CC}	
1421	1421	1410	ν_{10}	ν_{CC}	
1388	1387	1379	ν_{11}		$\beta_{CH(=O)}$
1304	1301	1309	ν_{12}	β_{CH}	
1293	1291	1270	ν_{13}	ν_{CC}	
1230	1227	1238	ν_{14}	ν_{C-F}	
1204	1202	1183	ν_{15}	$\nu_{C-C(=O)}$	
1150	1148	1133	ν_{16}	β_{CH}	
1095	1097	1080	ν_{17}	β_{CH}	
1012	1011	990	ν_{18}	β_{CH}	
859	858	839	ν_{19}	ν_{CC}	
774	772	757	ν_{20}		$\beta_{C(=O)}$
635	633	621	ν_{21}	α_{CCC}	
599	598	587	ν_{22}	α_{CCC}	
422	424	407	ν_{23}	α_{CCC}	
	383	372	ν_{24}	β_{C-F}	
	207	193	ν_{25}	$\beta_{C-C(=O)}$	
1003	999	993	ν_{26}		$\gamma_{CH(=O)}$
970		944	ν_{27}	γ_{CH}	
947		916	ν_{28}	γ_{CH}	
834	833	815	ν_{29}	γ_{CH}	
		801	ν_{30}	γ_{CH}	
705	704	681	ν_{31}	δ_{CC}	
506	505	498	ν_{32}	δ_{CC}	
		415	ν_{33}	δ_{CC}	
	336	324	ν_{34}	γ_{C-F}	
	190	187	ν_{35}	$\gamma_{C-C(=O)}$	
100[d]		99	ν_{36}		$\tau_{C-C(=O)}$

Wavenumber [cm^{-1}] — Approximate description[a]

[a] ν_{CX}: C—X stretching; β_{CX}: C—X in-plane bending; γ_{CX}: C—X out-of-plane bending; α_{CCC}: ring in-plane bending; δ_{CC}: ring out-of-plane bending. [b] B3LYP/6-31G*; scale factors of 0.96.[29] [c] Calculated values for dimer **1**. [d] According to ref. [23].
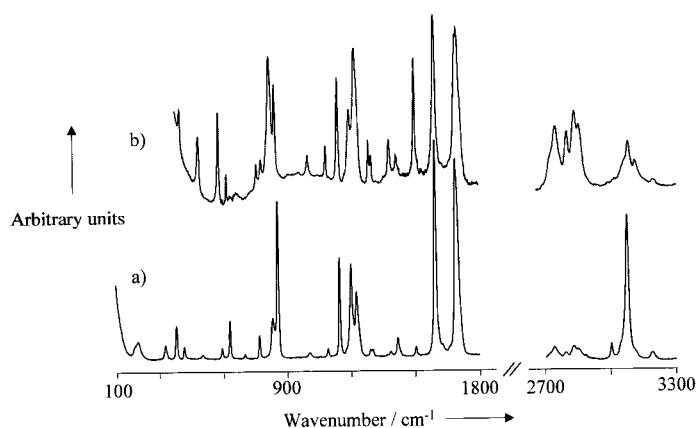
Figure 3. *Vibrational spectra of 4FB in the 100–1800 and 2700–3300 cm⁻¹ regions: a) Raman and b) FTIR.*

stretching bands present clear evidence of dimer–monomer splitting, as will be discussed below, and their proposed assignment is included in Table 3. It should be mentioned that the presence of pairs of closely overlapping bands related to other C—H and C=O modes (for example, out-of-plane bending modes) was suggested by dilution and temperature variation studies, but the weakness and/or strength of the overlap of such bands does not allow a definite conclusion to be drawn.

Table 4 presents some relevant vibrational wavenumbers and NMR chemical shifts (relative to the monomer) of the dimers **1** to **5**, calculated at the B3LYP/6-31G* level. As expected, the engagement of the C=O group in hydrogen bonding led to a red-shift of the $\nu_{C=O}$ mode, from -14 to -38 cm⁻¹, depending on the dimer considered. The same effect was predicted for the ν_{C-F} mode (dimer **4**), although with a lower magnitude

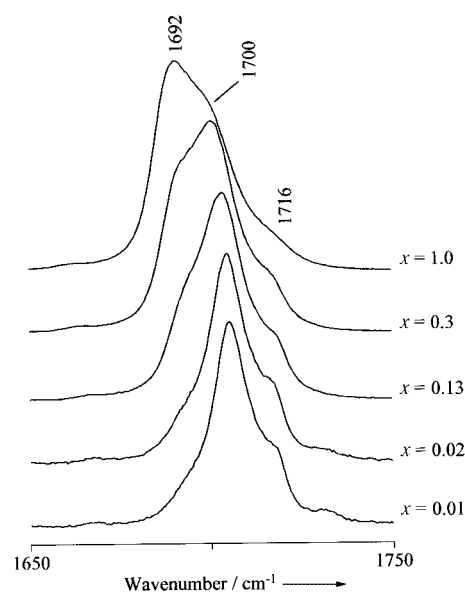$(-18$ cm⁻¹). On the other hand, the effect on the ν_{C-H} modes was more dependent on the nature of the donor, and both positive (blue) and negative (red) shifts were predicted. Whereas the C_7—H···O interactions led to larger blue-shifts (up to $+97$ cm⁻¹ in dimer **2**) the predicted shifts for the ring ν_{C-H} modes were positive for dimers **1** and **5**, and negative for dimers **2** and **4**.

The largest NMR shifts upon dimerization were predicted for the oxygen nuclei, whereas almost negligible shifts were predicted for the hydrogen nuclei. This is in agreement with experimental reports of 10–20 ppm shielding for the carbonyl oxygen atom when hydrogen bonded to OH groups, and of a 1–2 ppm deshielding for the C—H hydrogen atom interacting with strong proton acceptors.[18–20] Nonnegligible shifts were also predicted for the fluorine nuclei in dimer **4** and for the carbonyl carbon nuclei that belong simultaneously to a C—H donor and a C=O acceptor (dimers **2** and **3**).

Spectroscopic Study of the Effects on the Acceptor Fragment

The most evident spectroscopic effect of the hydrogen bonding in benzaldehyde molecules, including 4FB, is the splitting of the vibrational band corresponding to the carbonyl stretching mode ($\nu_{C=O}$). In the past, this splitting was assigned to Fermi resonance.[21] However, for 4FB, of the three bands observed in the $\nu_{C=O}$ region, only the shoulder at 1716 cm⁻¹ presents a behavior consistent with Fermi resonance (Figures 4 and 5). In the case of the 1692/1700 cm⁻¹ band pair, such an assignment is not supported by the observed intensity changes upon dilution and temperature variation, as will be discussed below, and the two bands have been ascribed to the bonded and free carbonyl groups, respectively.

Figure 4 presents the Raman spectra, in the $\nu_{C=O}$ region (1650–1750 cm⁻¹), of 4FB solutions in CCl₄ ($\varepsilon = 2.2$) at different

Table 4. *Calculated dimer–monomer differences for both the vibrational stretching modes [cm⁻¹] and the NMR chemical shifts [ppm] upon dimerization. Only the largest shifts are shown in each case for simplicity. Atom nomenclature is in accordance with Figure 1.*

		1	2	3	4	5
Vibrational mode[a]						
ν_1	$(C_{2,3}-H)_s$	$+6$	-2	-1	-2	-3
ν_2	$(C_{5,6}-H)_s$	$+1$	-12	0	-23	$+16$
ν_3	$(C_{2,3}-H)_{as}$	$+9$	-1	-1	$+1$	-2
ν_4	$(C_{5,6}-H)_{as}$	-2	$+8$	$+4$	$+4$	$+18$
ν_5	(C_7-H)	$+6$	$+97$	$+83$	$+69$	$+19$
ν_6	$(C=O)$	-14	-31	-38	-22	-13
ν_{14}	$(C-F)$	$+4$	$+3$	-2	-18	$+4$
Nuclei						
O		26	24	10	23	25
F		-1	0	1	8	-3
C_1		0	-1	-1	-1	0
$C_{2,6}$		-4	-3	1	-1	-3
$C_{3,5}$		-2	0	0	-3	-3
C_4		0	0	0	0	0
C_7		-2	-7	-7	-3	-2
$H(C_{2,6})$		-2	-1	-1	-1	-1
$H(C_{3,5})$		0	0	0	-1	-1
$H(C_7)$		0	-1	-1	0	0
[a] Numbering scheme in accordance with Table 3						

Figure 4. *Room temperature Raman spectra of 4FB/CCl₄ solutions with different mole fractions in the region of the C=O stretching modes.*
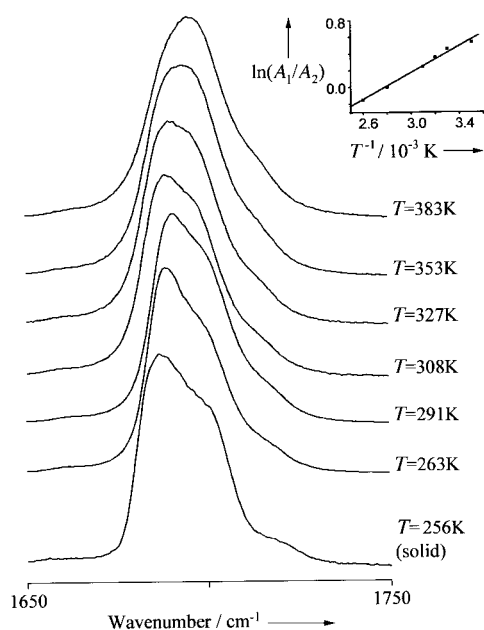
Figure 5. *Raman spectra of pure 4FB at several temperatures in the region of the C=O stretching modes. Inset: Logarithm of the intensity ratio versus the reciprocal of the temperature for the 1692/1700 cm^{-1} band pair is also shown.*

mole fractions. Other solvents, such as CH$_3$CN ($\varepsilon = 36.6$), C$_6$H$_{14}$ ($\varepsilon = 1.9$), C$_6$D$_6$ ($\varepsilon = 2.3$), and CH$_3$OH ($\varepsilon = 32.6$), were also used. Apart from the shifts expected due to solvent polarity, the effect of dilution in nondonor solvents was always found to be an intensity increase of the 1700 cm^{-1} (free $\nu_{C=O}$) band compared to the 1692 cm^{-1} (bonded $\nu_{C=O}$) band. Methanol, as a strong hydrogen-bond donor solvent, showed a relative intensification (with broadening) of the 1692 cm^{-1} band. This observation further supports the assignment of the 1692 cm^{-1} band to the hydrogen-bonded carbonyl group.

Figure 5 displays the temperature variation study, ranging from 256 K to 383 K, of pure 4FB over the same spectral region (1650 – 1750 cm^{-1}). The spectral observations paralleled the effects observed upon dilution, that is, a temperature increase was followed by a decrease of the 1692/1700 cm^{-1} band intensity ratio. This ratio is related to the dimerization equilibrium, but its use for determining the corresponding $\Delta H_{\text{dimerization}}$ value has some limitations. For instance, the evaluation of the dimer:($2 \times$ monomer) ratio from the 1692 – 1700 cm^{-1} band intensities requires the assumption that, in each dimer, both carbonyl groups are involved in hydrogen bonding, as single bonded dimers also contribute to the 1700 cm^{-1} "monomer" band. However, a simpler and straightforward estimate of the ΔH value for the dimerization can be obtained from the ratio between the *bonded* C=O$\cdots$ and the *free* C=O bands (corresponding to a C=O $\rightleftarrows$ C=O$\cdots$ equilibrium). The slope of the linear correlation between the logarithm of the intensity ratio versus the reciprocal temperature yielded a ΔH value of 6.7 ± 0.7 kJ mol^{-1}. This value is within the range of reported experimental values for C—H$\cdots$O hydrogen bonded systems.[10, 22]

The carbonyl ^{17}O NMR chemical shift (δ_{carbonyl}) is also sensitive to the presence of C—H$\cdots$O hydrogen bonds. In fact, the δ_{carbonyl}

of substituted benzaldehyde derivatives has been reported to move to higher field upon intra- or intermolecular hydrogen bonding.[10, 18, 19] Intermolecular hydrogen-type interactions involving O—H donors lead to shielding effects of the order of 10 – 18 ppm:[18, 19] Similar values have been found for intermolecular C—H$\cdots$O hydrogen bonds.[10] In 4FB, the observed shift for δ_{carbonyl}, from infinite dilution (monomer) to pure liquid (monomer plus dimer), is about 17 ppm. This unexpectedly large shift compares well with those observed for O—H$\cdots$O interactions, and it becomes apparent that δ_{carbonyl} can be used to identify the presence of hydrogen bonding but should not, however, be taken as a measure of the strength of such an interaction.

The above reported vibrational and NMR spectra present compelling evidence of the engagement of the carbonyl oxygen atom as a hydrogen bond acceptor in liquid 4FB, and show a reasonable agreement with the results obtained from ab initio calculations. In fact, the observed dimer – monomer vibrational splitting (8 cm^{-1}) is close to the 14 cm^{-1} predicted from ab initio calculations for dimer **1**, although well below the 38 cm^{-1} value predicted for dimer **3**. On the other hand, the calculated ^{17}O NMR dimerization shifts of about 23 – 26 ppm (except for **3**) are in accordance with the 17 ppm shift observed. Regarding the possible participation of the fluorine atom as a hydrogen bond acceptor, the experimental results point to a negligible contribution, in agreement with the ab initio calculations. In fact, all the vibrational bands assigned to C—F modes are single and symmetric, and the ^{19}F NMR spectrum is nearly insensitive to dilution.

### Spectroscopic Study of the Effects on the Donor Group

As previously mentioned, the most intriguing feature of the C—H$\cdots$O hydrogen bond is the predicted shortening of the C—H bond length in some dimer structures relative to the monomer.

In previous studies with benzaldehyde derivatives (4-methoxy- and 4-ethoxy-), a concentration-dependent broadening in the high wavenumber side of the formyl ν_{C-H} mode bands was observed.[10] These apparent blue-shifts have tentatively been assigned to C—H$\cdots$O hydrogen bonding. In the case of 2-methoxybenzaldehyde,[11] the presence of a C$_3$—H$\cdots$O hydrogen bond, identified by X-ray crystallography, gave rise to a $+21$ cm^{-1} blue-shift of the ν_{C_3-H} mode in the vibrational spectra. The two individual bands, related to the free and bonded ν_{C_3-H}, were ascribed in the vibrational spectra of both the solid and liquid phases.

Figure 6 compares the FTIR spectra, over the region of the ν_{C-H} modes, of pure 4FB and 4FB diluted in CCl$_4$ (a nonpolar solvent) and [D$_6$]acetone (a strong proton-acceptor solvent). As shown in Table 3, this region is comprised of two main groups of bands: the aromatic ν_{C-H} modes (above 2900 cm^{-1}) and the aldehydic ν_{C-H} ones (below 2900 cm^{-1}, with several Fermi resonance components).[23]

The analysis of the aldehydic ν_{C-H} mode is highly confounded by the multiple Fermi resonances, and no definite conclusions could be drawn from it. Nevertheless, from the diluted solution in CCl$_4$ to the solution in [D$_6$]acetone (that is, with the expected increase of the *bonded* C=O to *free* C=O ratio) there was an
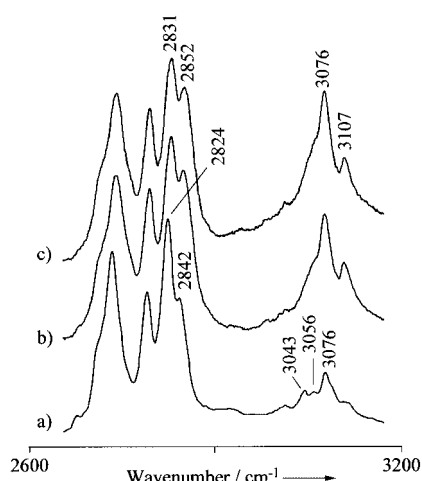
Figure 6. *Room temperature FTIR spectra of 4FB in the region of the C—H stretching modes: a) CCl₄ solution (x = 0.1), b) pure, c) [D₆]acetone solution (x = 0.1).*

intensity increase in the high wavenumber band of this region, and a overall blue-shift of the multiplet of about 7 cm^{-1}. The same effects, to a minor extent, were also observed upon decreasing the temperature.

A somewhat clearer situation arises for the ring ν_{C-H} modes. As can be seen from Figure 6, an increase of the bonded C=O to free C=O ratio (from Figure 6a to 6c) was followed by two main effects: 1) an overall enhancement of the ring ν_{C-H} bands relative to the aldehydic ν_{C-H} region; and 2) an intensity transfer from the 3043 cm^{-1} band to the 3107 cm^{-1} band. According to the ab initio calculations, the four ring ν_{C-H} modes of the monomer can be related to the four bands below 3100 cm^{-1}. This leaves out the 3107 cm^{-1} band, which was assigned to the bonded $\nu_{C-H(\cdots O)}$ mode, in accordance with its concentration dependent intensity. Since the 3043 cm^{-1} monomer band is related to the symmetric stretching of the $C_{2,3}$—H bonds, one may expect that dimers **1** and **2** are among the most significant (with longest lifetime) dimer forms in the liquid.

It has been shown[3, 20] that the proton-donating ability of a C—H bond can only be observed by ^{1}H NMR when this interaction occurs with strong proton acceptors in sterically favorable circumstances. In such cases, the observed downfield shift is about 1–2 ppm,[20] but becomes unobservable in the case of weaker interactions. On the other hand, several studies have focused on the relationship between C—H⋯X hydrogen bonding and C—H nuclear magnetic coupling (quantified by coupling constant, $^1J_{CH}$, values).[9, 20, 24] It has been suggested that the increase in $^1J_{CH}$ for a C—H bond near either a fluorine atom or a carbonyl oxygen is evidence of the presence of a C—H⋯F or C—H⋯O hydrogen bond, respectively.[9, 13, 20] The observed increase ranges from about 10 Hz, in thiophene carbaldehydes (O=C—H⋯O=C interaction),[20] to 3.7 Hz, in a triptycene derivative (C(sp³)—H⋯F interaction).[9] These values refer to intramolecular hydrogen bonding, and smaller values were found in C—H⋯O intermolecular hydrogen bonding in liquids.[10]

For 4FB, the concentration increase leaves the $^1J_{CH}$ for the ring $C_{3,5}$—H nuclei nearly unchanged, whereas it increases the $^1J_{CH}$ values of the $C_{2,6}$—H and C_7—H nuclei by 2.1 and 2.4 Hz, respectively (values extrapolated to infinite dilution). Moreover, since the values obtained for $C_{2,6}$—H are in fact an average for the bonded and nonbonded C—H donors, the C_2—H bond turns out to be the preferred C—H donor in 4FB.

Conclusions

According to the ab initio calculations performed, the most efficient hydrogen bonds in 4FB are those between the carbonyl oxygen proton-acceptor and the C_2—H and C_7—H proton-donors, as found in dimers **1** and **2**. The predicted energy of the interaction is within the range of the values reported for C—H⋯O hydrogen bonds.

The presence of a dimerization equilibrium in liquid 4FB is strongly supported by the vibrational and NMR spectroscopy results. In addition, the experimental results are in agreement with the predicted preferred donor and acceptors for hydrogen bonding.

With regard to the acceptor atom, both the wavenumber shift of the $\nu_{C=O}$ mode, and the $\delta_{carbonyl}$ (^{17}O) NMR shift observed from infinite dilution to pure liquid reflect the engagement of the oxygen atom as hydrogen bond acceptor. It should be mentioned that in the case of 4-methoxy- and 4-ethoxybenzal-dehyde, the magnitude of both the $\nu_{C=O}$ and $\delta_{carbonyl}$ shifts have been found to be related to ΔH value for the dimerization.[10] As can be seen in Table 5, this relation does not hold for 4FB, and the magnitude of the shifts cannot be used as a direct measure of the strength of the hydrogen bond interaction.

With regard to the C—H donor, the most interesting results are those relating the C—H⋯O hydrogen bond to the shortening of the C—H bond length of the C_2—H and C_7—H donors. The increase of the corresponding $^1J_{CH}$ values, by about 2.1 and 2.4 Hz, respectively, with an increase in the dimer:monomer ratio, is direct evidence of this effect.

Somewhat more controversial are the observations in the ν_{C-H} region of the vibrational spectra. The concentration-driven intensity transfer from the 3043 cm^{-1} band to the 3017 cm^{-1} band suggests the assignment of those bands to the free and bonded ν_{C-H} modes involving the C_2—H fragment, respectively. However, a word of caution is required, since the blue-shifting effect is not yet well characterized.

Table 5. *Comparison of spectroscopic and energetic C—H⋯O related parameters for some substituted benzaldehyde derivatives.*

Molecule	$\Delta\nu$ [cm^{-1}]	ΔH [kJ mol^{-1}]	$\Delta E^{[a]}$ [kJ mol^{-1}]	$\Delta(\delta_{carbonyl})$ [ppm]
4MeOB[b]	14	7.6 ± 0.9	7.5[c]	15
4EtOB[d]	10	5.7 ± 0.5	6.5	12
4FB	8	6.7 ± 0.7	8.6	17
2MeOB[e]	17	3.3 ± 0.5	5.0	–

[a] Energy of the dimer form equivalent to **2** in 4FB (B3LYP/6-31G*). [b] 4-methoxybenzaldehyde; ref. [10a]. [c] Calculated in this work. [d] 4-ethoxy-benzaldehyde; ref. [10b]. [e] 2-methoxybenzaldehyde; ref.[11].

Experimental

4FB and the solvents (Fluka or Aldrich) were used without further purification.

The Raman spectra were recorded on a Jobin-Yvon T64000 triple monochromator Raman system (focal length 0.640 m, aperture *f*/7.5) with a nonintensified CCD detector and an Ar$^+$ laser as the excitation source. An integration time of 5 s, and two scans were used for all the spectra. Samples were sealed in Kimax glass capillary tubes (0.8 mm i.d.). Temperature variation studies over the 177 – 383 K range were carried out with a homemade Harney – Miller-type assembly,[25] and the temperature was monitored by the resistivity of a calibrated thermocouple. Under these circumstances, the error in temperature is estimated to be less than 0.5 K, with fluctuations during each recording of not larger than 1 K.

The infrared spectra of liquid samples at room temperature were recorded over the 400 – 4000 cm^{-1} region on a Mattson 7000 FTIR spectrometer using a globar source, a deuterated triglycine sulfate (DTGS) detector and KBr windows. Each spectrum was composed of 32 scans, with a resolution of 1 cm^{-1} to a 7468 data point file, and was subjected to triangular apodization.

For the evaluation of band intensity ratios, integrated band intensities were determined by band fitting procedures, using Lorentzian functions.

The NMR spectra were obtained using a Fourier transform spectrometer (Unity-500 (Varian) operating at external magnetic fields of 2.97, 1.60, and 11.1 T, respectively, for ^{13}C, ^{17}O, and ^{19}F), in a 5 mm broadband probe at 298 K. For the ^{13}C NMR experiments, recorded without proton decoupling, the CCl_4 peak was used as the internal reference ($\delta = 96.7$ ppm). The ^{17}O and ^{19}F NMR spectra were obtained using D_2O and $CFCl_3$ as the external references ($\delta = 0$ ppm), respectively. Typically, spectral widths of 20 000 Hz, acquisition times of 0.4 s, and pulse delays of 8 – 12 s were used when obtaining ^{13}C and ^{19}F data. For ^{17}O spectra (recorded with a standard Cyclops pulse sequence) the corresponding parameters were 50 000 Hz, 60 ms, and 0.032 ms (90°). The chemical shifts obtained have an accuracy of ±1 ppm.

All ab initio calculations were performed on a PC computer, using the Gaussian 98w package.[26] The molecular structures of the monomer and dimers were fully optimized at the HF/6-31G* and B3LYP/6-31G* standard levels[27] using the gradient method. In particular, the B3LYP/6-31G* level has proven to be quite adequate for studying 4FB, as good agreement was obtained between the calculated structural parameters of the monomer and the experimental (gas-phase diffraction and microwave) and theoretical MP2/6-31G* results reported by Samdal et al.[28] For instance, the structural differences observed were always less than 2 pm and 2°, for bond lengths and angles, respectively. Additional calculations at the MP2/6-31G** level were performed for selected dimer structures, in order to evaluate the importance of the dispersion energy term.

Harmonic vibrational wavenumbers were calculated at the B3LYP level, using analytical second derivatives to confirm the convergence to minima on the potential surface, and to evaluate the ZPVE. The calculated wavenumbers were always scaled by a factor of 0.96.[29] The BSSE correction for the dimerization energies was estimated by counterpoise calculations[30] using the MASSAGE option of Gaussian 98.[26]

NBO analyses[31] were carried out in order to obtain a deeper insight into the electronic structures of the optimized geometries. The natural charges and the Wiberg bond indices based on the NAO Fock matrix were used to investigate the nature of the hydrogen bonding in the treated structures. The second order perturbation energy yielded valuable information concerning the type and strength of the intermolecular interactions.

All calculated NMR results reported in the present study are based on the GIAO (gauge including atomic orbitals) formulation[32] as implemented in Gaussian 98w.[26] The B3LYP/6-31G* level was used, as only relative dimer-to-monomer chemical shifts were required. In fact, tests performed with the B3LYP/6-311(d,p) basis set,[14] showed that the calculated relative chemical shifts due to dimerization are insensitive to the basis set used (either B3LYP/6-31G* or B3LYP/6-311(d,p)).

[1] G. A. Jeffrey, W. Saenger, *Hydrogen Bonding in Biological Structures*, Springer-Verlag, Berlin, **1991**, and references therein.

[2] G. R. Desiraju, T. Steiner, *The Weak Hydrogen Bond in Structural Chemistry and Biology*, Oxford University Press, New York, NY, **1999**, and references therein.

[3] M. Nishio, M. Hirota, Y. Umezawa, *The CH/π Interaction: Evidence, Nature, and Consequences*, Wiley-VCH, New York, NY, **1998**, and references therein.

[4] G. R. Desiraju, *Nature* **2001**, *412*, 397.

[5] Y. Gu, T. Kar, S. Scheiner, *J. Am. Chem. Soc.* **1999**, *121*, 9411.

[6] E. Cubero, M. Orozco, P. Hobza, F. J. Luque, *J. Chem. Phys.* **1999**, *103*, 6394.

[7] a) R. Vargas, J. Garzas, D. A. Dixon, B. P. Hay, *J. Am. Chem. Soc.* **2000**, *122*, 4750; b) L. Turi, *J. Phys. Chem.* **1996**, *100*, 11 285; c) P. L. A. Popelier, R. F. W. Bader, *Chem. Phys. Lett.* **1992**, *189*, 542.

[8] P. Hobza, V. Špirko, Z. Havlas, K. Buchhold, B. Reimann, H.-D. Barth, B. Brutschy, *Chem. Phys. Lett.* **1999**, *299*, 180.

[9] C. Vizzioli, M. C. R. de Azua, C. G. Giribert, R. H. Contreras, L. Turi, J. J. Dannenberg, I. D. Rae, J. A Weigold, M. Malagoli, R. Zanasi, P. Lazzaretti, *J. Phys. Chem.* **1994**, *98*, 8858.

[10] a) N. Karger, A. M. Amorim da Costa, P. J. A. Ribeiro-Claro, *J. Phys. Chem. A* **1999**, *103*, 8672; b) M. P. M. Marques, A. M. Amorim da Costa, P. J. A. Ribeiro-Claro, *J. Phys. Chem. A* **2001**, *105*, 5292.

[11] P. J. A. Ribeiro-Claro, M. G. B. Drew, V. Felix, *Chem. Phys. Lett.* **2002**, *356*, 318.

[12] K. Mizuno, T. Ochi, Y. Shindo, *J. Chem. Phys.* **1998**, *109*, 9502.

[13] J. D. Chaney, C. R. Goss, K. Folting, B. D. Santarsiero, M. D. Hollingsworth, *J. Am. Chem. Soc.* **1996**, *118*, 9432.

[14] P. R. Rablen, S. A. Pearlman, J. Finkbinder, *J. Phys. Chem. A* **1999**, *103*, 7357.

[15] K. K. Baldridge, J. S. Siegel, *J. Phys. Chem. A* **1999**, *103*, 4038.

[16] A. Bagno, S. Gerard, J. Kevelam, E. Menna, G. Scorrano, *Chem. Eur. J.* **2000**, *6*, 2915.

[17] M. Bühl, M. Kaupp, O. L. Malkina, V. G. Malkin, *J. Comput. Chem.* **1999**, *20*, 91.

[18] Th. E. St. Amour, M. I. Burger, B. Valentine, D. Fiat, *J. Am. Chem. Soc.* **1981**, *103*, 1128.

[19] D. W. Boykin, S. Chandrasekaran, A. L. Baumstark, *Magn. Reson. Chem.* **1993**, *31*, 489.

[20] H. Satonaka, K. Abe, M. Hirota, *Bull. Chem. Soc. Jpn.* **1988**, *61*, 2031.

[21] R. A. Nyquist, *Appl. Spectrosc.* **1992**, *46*, 306.

[22] A. Goel, C. N. R. Rao, *J. Chem. Soc., Faraday Trans.* **1971**, 2828.

[23] J. H. S. Green, D. J. Harrison, *Spectrochim. Acta* **1976**, *32A*, 1265.

[24] A. V. Afonin, M. V. Sigalov, S. E. Korustova, I. A. Aliev, A. V. Vashchenko, B. A. Trofimov, *Magn. Reson. Chem.* **1990**, *28*, 580.

[25] F. A. Miller, B. M. Harney, *Appl. Spectrosc.* **1970**, *2*, 291.

[26] *Gaussian 98 (Revision A.7)*, M. J. Frisch, G. W. Trucks, H. B. Schlegel, G. E. Scuseria, M. A. Robb, J. R. Cheeseman, V. G. Zakrzewski, J. A. Montgomery, R. E. Stratmann, J. C. Burant, S. Dapprich, J. M. Millam, A. D. Daniels, K. N. Kudin, M. C. Strain, O. Farkas, J. Tomasi, V. Barone, M. Cossi, R. Cammi, B. Mennucci, C. Pomelli, C. Adamo, S. Clifford, J. Ochterski, G. A. Petersson, P. Y. Ayala, Q. Cui, K. Morokuma, D. K. Malick, A. D. Rabuck, K. Raghava-

chari, J. B. Foresman, J. Cioslowski, J. V. Ortiz, A. G. Baboul, B. B. Stefanov, G. Liu, A. Liashenko, P. Piskorz, I. Komaromi, R. Gomperts, R. L. Martin, D. J. Fox, T. Keith, M. A. Al-Laham, C. Y. Peng, A. Nanayakkara, C. Gonzalez, M. Challacombe, P. M. W. Gill, B. G. Johnson, W. Chen, M. W. Wong, J. L. Andres, M. Head-Gordon, E. S. Replogle, J. A. Pople, Gaussian, Inc., Pittsburgh, PA, **1998**..

[27] a) P. C. Hariharan, J. A. Pople, *Theor. Chim. Acta* **1973**, *28*, 213; b) A. D. Becke, *J. Chem. Phys.* **1993**, *98*, 5648; c) C. Lee, W. Yang, R. G. Parr, *Phys. Rev. B* **1988**, *37*, 785.

[28] S. Samdal, T. G. Strand, M. A. Tafipolski, L. V. Vilkov, M. V. Popik, H. V. Volden, *J. Mol. Struct.* **1997**, *435*, 89.

[29] A. P. Scott, L. Radom, *J. Phys. Chem.* **1996**, *100*, 16 513.

[30] S. F. Boys, F. Bernardi, *Mol. Phys.* **1970**, *19*, 553.

[31] *NBO (Ver. 3.1)*, E. D. Glendening, A. E. Reed, J. E. Carpenter, F. Weinhold.

[32] a) F. J. London, *Radium (Paris)* **1937**, *8*, 397; b) R. Ditchfield, *Mol. Phys.* **1974**, *27*, 789; c) K. Wolinski, J. F. Hinton, P. Pulay, *J. Am. Chem. Soc.* **1990**, *112*, 8251; d) M. Häser, R. Ahlrichs, H. P. Baron, P. Weiss, H. Horn, *Theor. Chim. Acta* **1992**, *83*, 455.